

Monitoring Low Frequency Propagation with a Software Defined Radio Receiver
Part I ~ Propagation Concepts
Whitham D. Reeve

I.1. Introduction

The effects of a solar flare on terrestrial radio propagation and thus the flare itself may be detected by monitoring variations in the signals received from a low frequency transmitter. The variations caused by a flare are called a *sudden ionospheric disturbance* or *SID* because of their transient effects on Earth's ionosphere.

This paper consists of two parts: Part I reviews low frequency propagation and how monitoring low frequency communication signals may be used to indirectly observe solar flares through SID detection, and Part II discusses the instrumentation and shows examples of signals received at Coho Radio Observatory (CRO) in Alaska from low frequency transmitters around the world. For purposes of this paper, *low frequencies* refer to frequencies in the VLF band (3 to 30 kHz) and lower part of the LF band (30 to 300 kHz) up to approximately 50 kHz. These low frequencies most often are used in secure one-way military submarine communications. The transmitters are located on land and typically use very large antenna systems requiring thousands of square kilometers land area and output powers up to about one megawatt.

The observations were produced by a software defined radio (SDR) receiver and an untuned square loop antenna with balanced feed. The propagation examples in this paper were recorded in the second half of 2018 as the sunspot cycle approached its minimum. Although the receiver and antenna system were built to detect sudden ionospheric disturbances, it is not surprising that no SIDs were detected at the time because of the low point in the sunspot cycle. However, the setup and observations described here provide a path for future investigations during the next solar cycle.

I.2. Earth-Ionosphere Waveguide Mode

This section is based on [Hunsucker], [{VLFRadio}](#) and [{Navelex}](#). Calculation procedures for predicting the received field strength at low frequencies are beyond the scope of this paper but are given in [\[ITU-P.684\]](#). In addition to these references, readers interested in low frequency radio wave propagation should see [{Wait}](#).

Terrestrial radio waves can propagate by various modes including *sky waves*, *space waves* and *ground waves* (figure I.1). Space waves, which are a combination of ground waves and multi-hop sky waves along the path, support low frequency propagation in what is called the Earth-ionosphere waveguide. The waveguide mode usually applies to low-incidence angle, low frequency propagation distances greater than 1000 km.

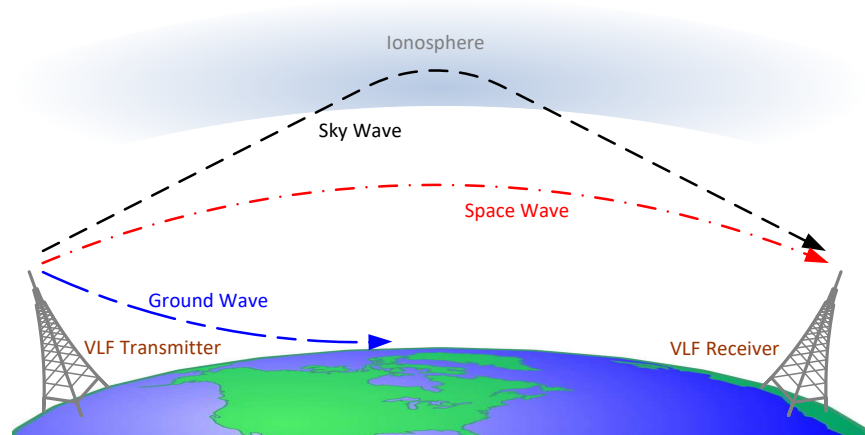


Figure I.1 ~ Possible propagation modes include sky wave, space wave and ground wave. Low frequency radio waves can travel considerable distances via ground waves and sky waves. Ground waves follow Earth's surface and eventually dissipate due to ground losses. Sky waves enter the ionosphere where they are refracted back toward Earth; sky waves eventually dissipate due to absorption in the lower part of the ionosphere. Even longer distances are possible when the low frequencies are propagated as space waves, which are combinations of ground waves and sky waves. Space waves use what is called the Earth-ionosphere waveguide mode in which the lower boundary of the waveguide is Earth's surface and the upper boundary is Earth's ionosphere. Image © 2018 W. Reeve

During the day, Earth's surface and the ionosphere's D-region form a concentric spherical waveguide, which supports the propagation of low frequency radio waves. The lower part of the waveguide is formed by the high conductivity of the ground or water surface and, during the day, the upper part is formed by the sharp change in refractive index in the ionosphere's D-region. Although *refraction* is the principle mechanism for low angle propagation, the term *reflection* is perhaps more intuitive and is used interchangeably throughout this paper.

The daytime D-region height ranges from about 60 to 75 km and the nighttime height ranges from about 75 to 95 km. The electron density and refractive index change significantly within a few tens of km, or on the order of about one wavelength at VLF. For reference, the free space wavelength of a 20 kHz radio wave is 15 km. The altitude at which the refraction takes place falls sharply, perhaps 15 km, before ground sunrise and remains almost constant during the day. The increase in electron density at sunrise is equivalent to a decrease in height and increase in the radio wave phase velocity. On the other hand, the refraction region rises sharply after ground sunset as the ionized gases at lower altitudes recombine and neutralize; the increase in height is equivalent to a decrease in phase velocity. These altitude changes at sunrise and sunset can significantly affect the received signal levels (figure I.2).

The Earth-ionosphere supports a number of waveguide modes depending on the height of the reflective regions and the frequency. In this case, modes describe the configuration of the electric and magnetic fields in the waveguide. When the wavelength exceeds the height of the reflecting boundary of the waveguide only zero-order transverse electric (TE) and transverse magnetic (TM) modes exist. *Transverse* means the electric or magnetic field is perpendicular to the direction of propagation. For shorter wavelengths (higher frequencies), a first-order mode generally dominates, for example, TM_{10} (figure I.3), but other lower order modes also exist, for example, TM_{20} and TM_{30} . Mode conversion can take place on long paths. Maximum attenuation in the waveguide during the day occurs when the wavelength equals the height of the reflecting layer, generally in the range of 75 to 100 km (frequency in the range 3 to 4 kHz). Attenuation decreases as the wavelength is reduced

until increasing radio wave penetration and associated absorption loss at the reflection boundaries cause the attenuation to increase.

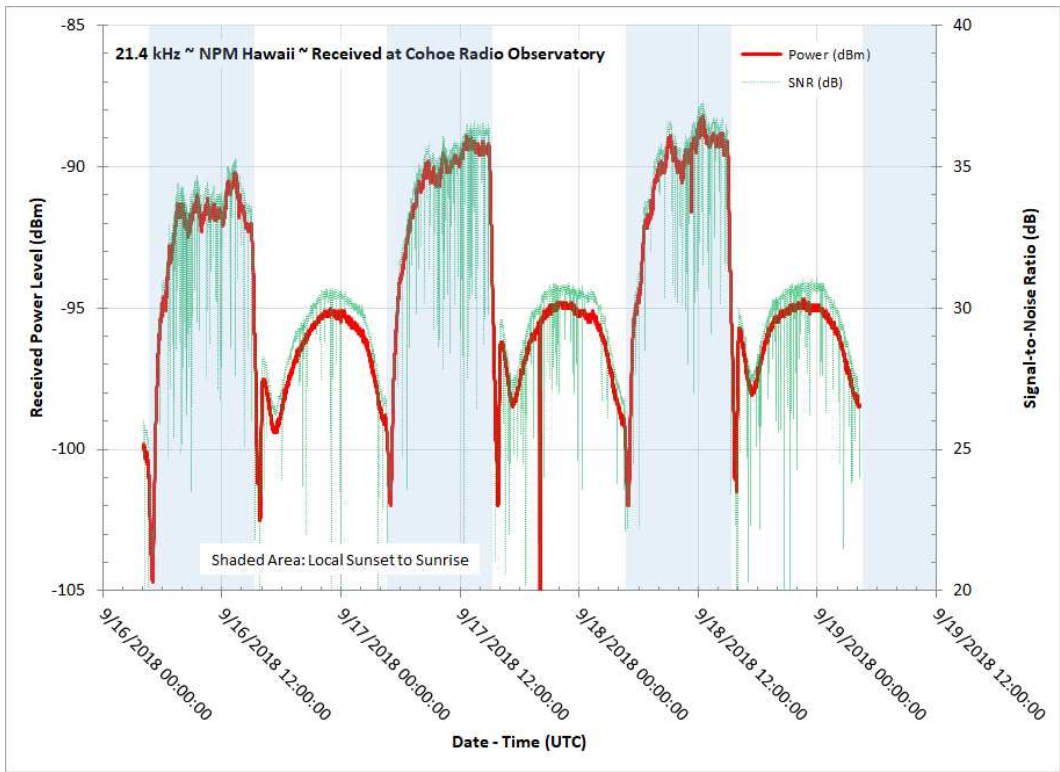


Figure I.2 ~ Received signal level (red trace, left axis) and signal-to-noise ratio (light green trace, right axis) for three days in mid-September 2018 on the 4390 km path from the Hawaiian station NPM transmitting on 21.4 kHz to a receiver at Cohoe Radio Observatory in Alaska. The dips in signal level at sunrise and sunset are clearly seen. These data were obtained near the autumnal equinox in which the split between day and night durations is almost equal. Image © 2018 W. Reeve

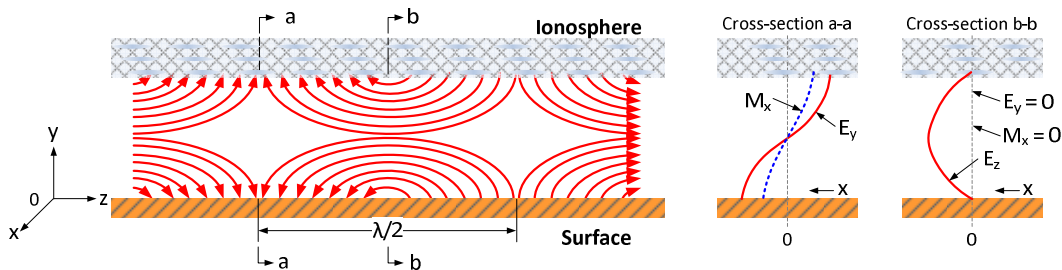


Figure I.3 ~ Electric (E) and magnetic (M) fields for the TM_{10} mode propagating between the ionosphere and Earth's surface, in which there is no magnetic field in the direction of propagation (propagation is along the z-axis shown here). Adapted from figure 3.4.2 in [{VLFRadio}](#).

At lower latitudes the D-region altitude remains almost constant or varies slowly during the day, so the received signal strength of low frequency radio waves also remains almost constant. Unvarying daytime signal strength is not as apparent at higher latitudes presumably because the D-region ionization follows a different pattern during the day and the effects of Earth's magnetic field are more pronounced. In any case, the signal strength is lower during the day than at night because during the day the radio waves penetrate the D-region on their way in and out as they propagate along the waveguide and lose some energy by absorption.

At night, the D-region electron density decreases and the sporadic E- and F-regions of the ionosphere may form the upper part of the waveguide and reflections may take place at heights above about 90 km. In this situation,

the radio waves experience less absorption loss as they pass through that part of the atmosphere considered to be the D-region. The reduction of ionization in the D-, E- and F-regions at night generally causes higher variations in received signal levels than during the day. Additional details on the formation of the ionosphere are provided in **Appendix I.1**.

Although the waveguide propagation mode enables relatively efficient propagation, the specific path and station characteristics heavily influence the path losses. The huge transmitting powers and antenna sizes of low frequency transmitting stations are indications of the additional losses involved in this type of propagation; for example, see the satellite view of station NAA (24.0 kHz) in Maine USA (figure I.4). Receiver antennas are quite small by comparison. The antenna often used in SID detectors is a simple loop with a characteristic dimension of about 1 m (figure I.5).

Some additional considerations for low frequency propagation are:

- ⊗ The transitions between land, water and ice and across the solar terminator (gray line or sunrise-sunset boundary) are equivalent to waveguide discontinuities and may enhance or degrade propagation;
- ⊗ Where the propagation distance $d \approx \pi \cdot r \approx 20000$ km (r = Earth's radius, 6370 km), receiver locations can experience enhancements due to convergence of numerous propagation paths around the spherical Earth. The phenomenon is called *antipodal focusing*. Interference patterns also may exist at locations near an antipode. An example of a near-antipodal path is given in Part II of this paper;
- ⊗ As the low frequency wave front progresses beyond 5000 km, it is no longer expanding but is converging, leading to positive and negative interference patterns;
- ⊗ The mix of day and night influences the ionosphere along the path. The mix changes with the seasons and over a 24 h period. Longer daylight hours in the northern hemisphere correspond to shorter daylight hours in the southern hemisphere. Stations at mid- and low-latitudes experience a more even split of day and night throughout the year than stations at higher latitudes. Higher latitude stations experience long days during summer and short days during winter;
- ⊗ Earth's magnetic field significantly influences the ionosphere and the way electrons respond to passing radio waves. The field lines have a low angle with respect to Earth's surface at lower latitudes but sharply dip at even moderately higher latitudes; for example, the magnetic dip angle (inclination) at CRO Alaska at latitude 60° N is 73° and at station NPM in Hawaii at latitude 21° N is 38°;
- ⊗ Polar paths encounter wide variations in magnetic field inclination. Several polar paths are discussed in Part II of this paper;
- ⊗ The transmitter and receiver antennas are short probes in the Earth-ionosphere waveguide, and their ability to couple radio energy into and out of the waveguide is determined by the antenna efficiencies, radiation patterns and local Earth losses. Transmitter antennas generally are quite efficient (often above 80%) because of their large physical extent while receiver antennas, because they are so much smaller, are extremely inefficient.

I.3. Solar Flare Effects on Low Frequency Propagation

A solar flare is an explosion on the Sun believed to be caused by the sudden release of energy stored in unstable magnetic fields, usually above a sunspot. Flares produce an intense burst of radiation across the electromagnetic spectrum, from radio waves through infrared, ultraviolet (UV), extreme ultraviolet (EUV) to x-rays and gamma-

rays. The radiation propagates at the speed of light and reaches Earth in a little more than eight minutes. Reported flare times use an Earth reference so a flare peak that is reported at, say, 1209 UTC actually occurred 8-1/3 min earlier. Solar flares have been studied scientifically for many years and are labeled according to an intensity or magnitude classification system, which is discussed in **Appendix I.2**.

When the flare radiation penetrates Earth's ionosphere, particularly into the D-region, it suddenly increases the amount of ionization, or electron density, and temperature. The temperature increase causes the ionosphere to expand and move. The D-region suddenly becomes a better reflector at low angles, which enhances low frequency propagation and usually leads to an increase in the signal strength received from a low frequency transmitter. Sometimes the signal level decreases rather than increases due to propagation effects along the path. In any case, a sudden change seen on a plot of signal strength with respect to time infers the occurrence of a SID and a solar flare.

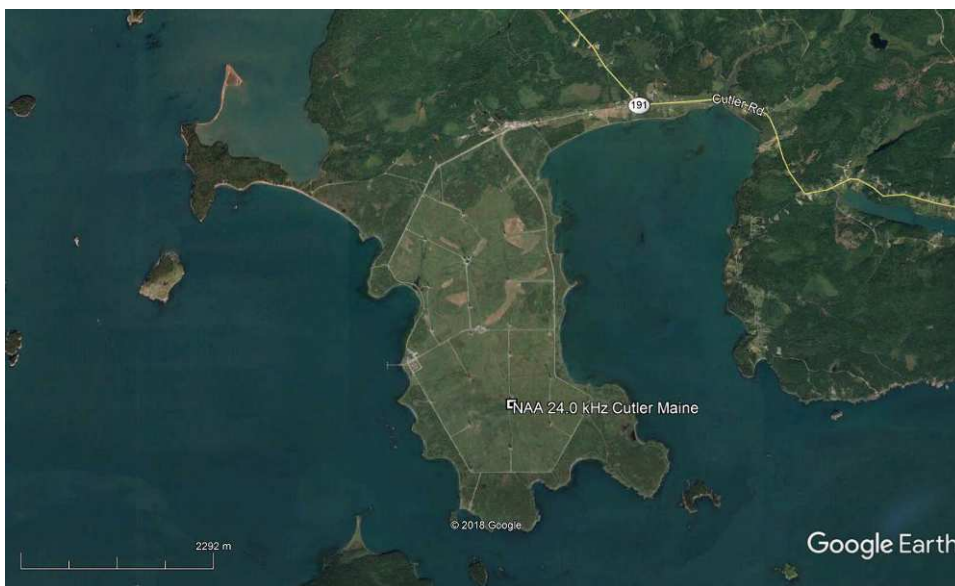


Figure I.4.a ~ Satellite image from 10 km altitude of the antenna site for station NAA (24.0 kHz) in Maine USA at coordinates 44°38'13.83"N, 67°16'41.99"W. The dimensions of the area occupied by the antenna are approximately 2 x 4 km, taking up the entire peninsula. North is up. Image source: Google Earth

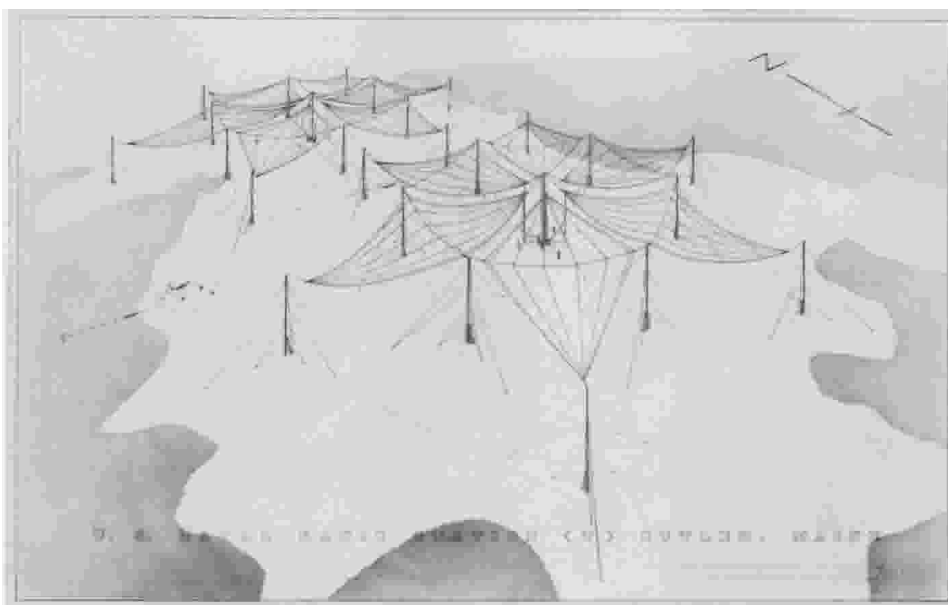


Figure I.4.b ~ Drawing of the NAA transmitter antenna near Cutler, Maine USA. Image source: Figure 2.8.11 in [{VLFRadio}](#)

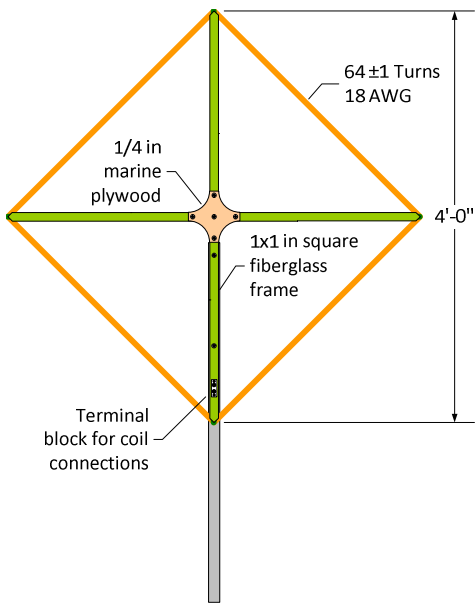


Figure I.5 ~ Typical small loop antenna used with low frequency receivers. The antenna shown here is installed at Cohoe Radio Observatory. It is wound with coated copper magnet wire on a fiberglass square tube frame and has an effective electrical height $h_e = 27 \text{ mm}$ at 24 kHz. Image © 2018 W. Reeve

The observed amplitude of a SID event usually can be correlated with the flare class or magnitude; however, the observed amplitude will depend on ionospheric conditions and receiver response and calibration. In amateur SID monitoring applications these will vary considerably among observers so measured *SID amplitudes* are not especially useful. On the other hand, *SID duration* and flare magnitude also are well correlated. The duration can be measured fairly consistently across many observers, so it is a useful metric. SIDs usually have a characteristic shark fin shape with a fast-rising leading edge and slow-decaying falling edge (figure I.6).

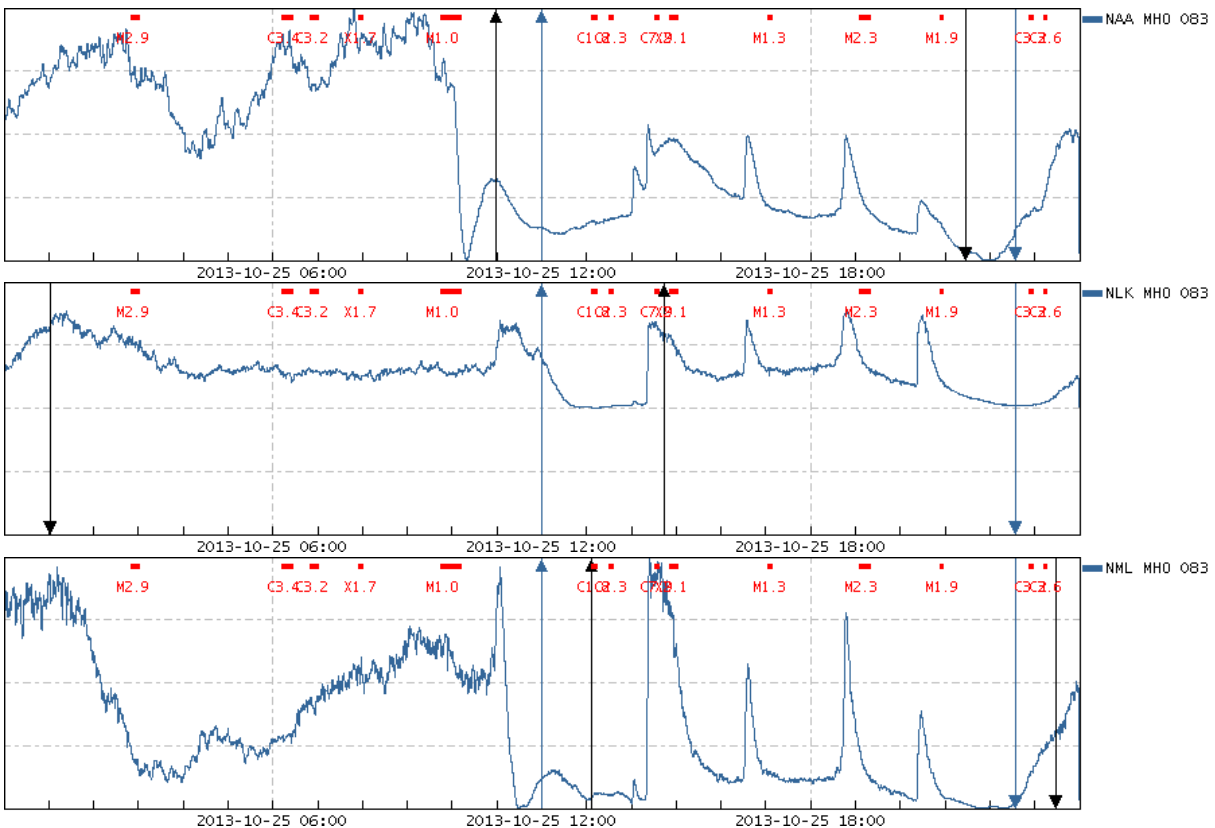


Figure I.6 ~ Three plots for 25 October 2013 of uncalibrated low frequency received signal level (vertical scale) with respect to time (UTC, horizontal scale). The transmitter sites are, top-to-bottom, NAA (24.0 kHz) in Maine, NLK (24.8 kHz) in Washington and NPM (21.4 kHz) in Hawaii; all are in USA. The receiver site is in Michigan USA. The black up-arrow indicates sunrise and the black down-arrow indicates sunset at the transmitter site in each plot. Similarly, the blue up- and down-arrows indicate sunrise and sunset at the receiver site. Relatively high, short-term signal variations occur during the night at the receiver site, especially between about 0000 and 1100 UTC. Except for station NLK, the received signal levels rise at night. Numerous solar flares are marked along the top of the plot, including several M-class (moderate) and one X-class (extreme) flares; some flares overlap. The corresponding SIDs with their signature shark-fin shape can be seen in the traces immediately below the flare labels. Image source: Stanford Solar Center [{SSCData}](#); receiver site maintained by Tom Hagen

I.4. Summary

Low frequencies in the range of interest (up to about 50 kHz) propagate via the Earth-ionosphere waveguide mode. This mode consists of space waves – combinations of ground waves and sky waves. The waveguide boundaries on the day side of Earth are Earth’s surface and the ionosphere’s D-region. On the night side, the D-region disappears and the boundaries are Earth’s surface and the ionosphere’s E- and F-regions. Propagation during the night incurs lower losses than during the day because there is no D-region to absorb the radio wave energy. The radiation from a solar flare quickly increases ionization in the D-region on Earth’s day side, which enhances propagation and produces a sudden ionospheric disturbance.

I.5. References and Weblinks

- [Hunsucker] Hunsucker, R. and Hargreaves, J., The High-Latitude Ionosphere and its Effects on Radio Propagation, Cambridge University Press, 2003
- [Kundu] Kundu, M., Solar Radio Astronomy, Wiley, 1965
- [[ITU-P.684](#)] Rec. ITU-R P.684-7, Prediction of field strength at frequencies below about 150 kHz, 10/2016, available at: <https://www.itu.int/rec/R-REC-P.684-7-201611-l/en>
- {[Navelex](#)} VLF, LF and MF Communication Systems, Navelex 0101,113, August 1972, available at: <http://navy-radio.com/manuals/shore-vlf.htm>
- {[VLFRadio](#)} Watt, A., VLF Radio Engineering, International Series of Monographs in Electromagnetic Waves, Vol. 14, Elsevier, 2018, available as paid download at: <https://www.elsevier.com/books/vlf-radio-engineering/watt/978-0-08-012313-4>
- {[Wait](#)} Wait, J. and Spies, K., Characteristics of the Earth-Ionosphere Waveguide for VLF Radio Waves, Technical Note No. 300, National Bureau of Standards, 30 Dec 29 1964, available for download at: <https://archive.org/details/characteristicso300wait>
- {[ReeveVLF](#)} http://www.reeve.com/Documents/Articles%20Papers/Reeve_VLF-LFStationList.pdf
- {[SSCData](#)} <http://sid.stanford.edu/database-browser/>

Appendix I.1 ~ Earth's Ionosphere

At the higher altitudes in Earth's atmosphere, about 1000 km, solar radiation is very strong even from the quiet Sun. This intense radiation covers a broad spectrum range from radio through infrared (IR), visible light, ultraviolet (UV), extreme ultraviolet (EUV), to x-rays and gamma-rays. Solar radiation at ultraviolet, extreme ultraviolet and higher frequencies (shorter wavelengths) is ionizing because photons at these frequencies have enough energy to dislodge an electron from a neutral oxygen gas atom or molecule during a collision (figure I.1.1). A photon is a particle that represents a quantum of electromagnetic radiation and whose energy is proportional to its frequency. The ionosphere has the properties of both a thin gas and plasma. Plasma is a cloud of charged particles – positive ions and free electrons – but has an overall neutral electrical charge.

See section I.4 for references

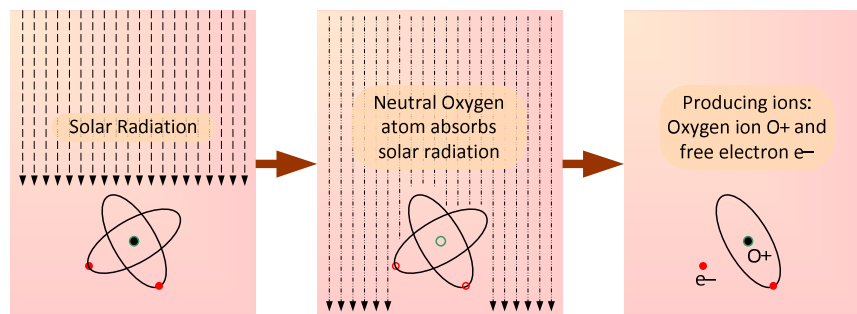


Figure I.1.1 ~ Radiation from the Sun dislodges electrons from Oxygen atoms and molecules in Earth's upper atmosphere producing the ionosphere. A solar flare produces higher energy photons, which penetrate deeper into the atmosphere and increase the ionization and, thus, the electron density in the D-region.

As the radiation penetrates Earth's atmosphere, it encounters more gas atoms at lower altitudes and the ionization process increases. However, an opposing recombination process takes place at the same time, in which free electrons are captured by nearby positive ions. At lower altitudes, where the gas density is higher, more recombination takes place because the gas molecules and ions are closer together. The balance between these ionization and recombination processes determines the amount of ionization at any given time and altitude.

At still lower altitudes, the atom (and molecule) density increases further and they have more opportunity to absorb the energy from a photon of ultraviolet solar radiation. However, the intensity of this radiation is lower at these lower altitudes because some of its energy was already absorbed at higher altitudes. A point is reached where lower radiation, greater gas density and greater recombination rates balance out and the ionization decreases with decreasing altitude. As a result, the ionosphere is negligible below about 60 km altitude. Thus, the beginning of the ionosphere from the standpoint of Earth's surface is at an altitude of about 60 km. The varying amounts of ionization at different altitudes lead to the formation of ionization layers or regions called D, E, F1, and F2 (table I.1.1).

The levels of ionization are different on Earth's night and day sides. Ionization also depends on the sunspot cycle (figure I.1.2) and summer and winter seasons. The D-region, which is the lowest region in the ionosphere, disappears completely at night. The higher E- and F-regions can remain for a few hours at night but dissipate as recombination takes place with no offsetting ionization by the Sun's radiation. The E-region may continue

sporadically (sporadic-E) at night while the F1- and F2-regions merge and are simply called the F-region. The ionosphere does not completely disappear at night because cosmic rays continue to bombard the upper atmosphere and form ions. Cosmic rays also are present on Earth’s day side but their influence is negligible compared to the Sun’s.

Table I.1.1 ~ Ionosphere layers. The amount of ionization is indicated by the electron density

Layer	Altitude range (km)	Electron density (electrons m ⁻³)
D	60 – 90	10 ⁸ – 10 ¹⁰
E	105 – 160	10 ¹¹
F1	160 – 180	10 ¹¹ – 10 ¹²
F2	up to 300	10 ¹²

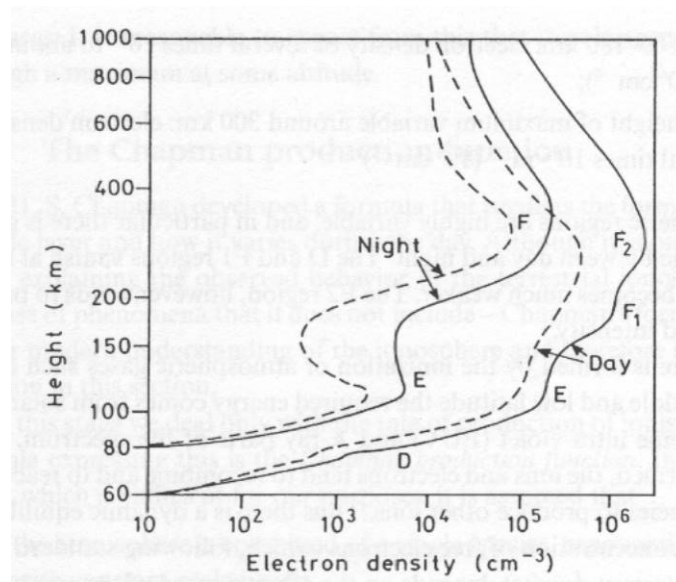


Figure I.1.2 ~ Day and night ionosphere regions. Solid line: Sunspot maximum; Dashed line: Sunspot minimum. Source: Fig. 1.4 [Hunsucker]

Appendix I.2 ~ Solar Flares

Flare classifications: Solar flares are classified according to their x-ray brightness (power density) in the wavelength range 0.1 to 0.8 nm. There are three main categories and two additional subsidiary categories, in ascending order of magnitude: A, B, C, M and X. Each category is separated by a power of ten in peak power density (Table I.2.1). Most scales list only C, M and X. The two lowest scales, A and B, represent a quiet Sun.

See section I.4 for references

The three highest categories have nine subdivisions ranging from 1 to 9, as in C1 to C9, M1 to M9, and X1 to X9. The subdivisions indicate a multiplier. For example, a flare categorized as C7 has a peak power density of 7 x 10⁻⁶ w m⁻² and M2 has a peak power density of 2 x 10⁻⁵ w m⁻².

X-class flares are the most powerful and can trigger worldwide radio blackouts and long-lasting radiation storms that are dangerous to spacecraft and space travelers. M-class flares are medium-sized and can cause brief radio

blackouts that affect communications in Earth's Polar Regions. Minor radiation storms sometimes follow an M-class flare. Compared to X- and M-class events, C-class flares are small with few noticeable effects on Earth. The A- and B-class flares are thought to have negligible effect on Earth but their long-term effects are not fully understood. Generally, X-, M- and C-class flares are detectable with a SID monitor as are some of the more energetic B-class flares.

Table I.2.1 – Solar flare classification

Class	Peak power density ($w m^{-2}$)
A	$I < 10^{-7}$
B	$10^{-7} \leq I < 10^{-6}$
C	$10^{-6} \leq I < 10^{-5}$
M	$10^{-5} \leq I < 10^{-4}$
X	$10^{-4} \leq I$

As already discussed low frequency receivers measure the amplitude of a received signal, not the power density of a flare. However, the change in amplitude and the duration of that change are related to flare magnitudes so the low frequency receiver provides an indirect flare measurement system.

Flare magnitude measurement: The total energy in a flare depends on its area, duration and intensity. Flare areas can vary over a wide range but duration and intensity vary over a relatively small range. Also, duration and intensity are loosely correlated with area. Flare magnitudes are estimated on a scale of *Importance* based on flare heliographic area (Table I.2.2). The Importance scale is a rough index conceived in 1955 by the International Astronomical Union. It is rough because a flare’s form, brightness and spectrum vary with time in a complex way.

Table I.2.2 – Importance classification of flares. Source: [Kundu]

Importance	Heliographic area (10^{-6} visible hemisphere)	H α line width (nm)	H α Intensity center (nm)	Relative frequency of occurrence
-1	< 100	0.15	0.06	---
1	100 – 250	0.30	0.08 – 0.15	0.72
2	250 – 600	0.45	0.12 – 0.20	0.25
3	600 – 1,200	0.80	0.14 – 0.25	0.03
3+	> 1,200	1.50	0.20 – 0.30	---

The complete Importance scheme includes two sub-classifications 1+ and 2+. The area-based classification 1, 2 or 3 is changed by one or two steps up or down when the intensity or hydrogen alpha (H α) line width is exceptional.



Author - Whitham Reeve is a contributing editor for the SARA journal, Radio Astronomy. He obtained B.S. and M.S. degrees in Electrical Engineering at University of Alaska Fairbanks, USA. He worked as a professional engineer and engineering firm owner/operator in the airline and telecommunications industries for more than 40 years and now manufactures electronic equipment used in radio astronomy. He has lived in Anchorage, Alaska his entire life. Email contact: whitreeve@gmail.com

Document Information

Author: Whitham D. Reeve

Copyright: ©2019, 2020 W. Reeve

Revisions: 0.0 (Original draft pulled from Cohoe VLF paper, 21 Aug 2018)

0.1 (Developed propagation description, 25 Sep 2018)

0.2 (Added images, 27 Sep 2018)

0.3 (Numerous minor edits, 07 Oct 2018)

0.4 (Added image for waveguide mode TM, 09 Oct 2018)

0.5 (Preparation for distribution, 23 Jan 2019)

0.6 (Minor edits prior to distribution, 26 Jan 2019)

0.7 (Minor edits for distribution, 19 Feb 2019)

0.8 (Minor edits to section 1.2, 18 Jan 2020)

Word count: 3852

File size (bytes): 4771328